

On Signal Peak Power Constraint of Over-the-Air Federated Learning

Lorenz Bielefeld[†], Paul Zheng^{*}, Oner Hanay[§], Yao Zhu^{*}, Yulin Hu^{‡*}, and Anke Schmeink^{*}

^{*}Chair of Information Theory and Data Analytics, RWTH Aachen University, Germany.

Email: zheng|zhu|schmeink@inda.rwth-aachen.de

[†]RWTH Aachen University, Germany. Email: lorenz.bielefeld1@rwth-aachen.de

[‡]School of Electronic Information, Wuhan University, China. Email: yulin.hu@whu.edu.cn

[§]InCirT GmbH, Germany.

Abstract—Federated learning (FL) has been considered a promising privacy preserving distributed edge learning framework. Over-the-air computation (AirComp) technique leveraging analog transmission enables the aggregation of local updates directly over-the-air by exploiting the superposition properties of wireless multiple-access channel, thereby drastically reducing the communication bottleneck issues of FL compared with digital transmission schemes. This work points out that existing AirComp-FL overlooks a key practical constraint, the instantaneous peak-power constraints imposed by the non-linearity of radio-frequency power amplifiers. We present and analyze the effect of the classic method to deal with this issue, amplitude clipping combined with filtering. We investigate the effect of instantaneous peak-power constraints in AirComp-FL for both single-carrier and multi-carrier orthogonal frequency-division multiplexing (OFDM) systems. We highlight the specificity of AirComp-FL: the samples depend on the gradient value distribution, leading to a higher peak-to-average power ratio (PAPR) than that observed for uniformly distributed signals. Simulation results demonstrate that, in practical settings, the instantaneous transmit power regularly exceeds the power-amplifier limit; however, by applying clipping and filtering, the FL performance can be degraded. The degradation becomes pronounced especially in multi-carrier OFDM systems due to the in-band distortions caused by clipping and filtering.

Index Terms—FL, over-the-air computation, peak-to-average, peak power constraint.

I. INTRODUCTION

An unprecedented volume of data is now generated at the wireless edge. Leveraging these data to train machine learning models at a centralized server is challenged by privacy concerns and limited uplink bandwidth requirements. Federated learning (FL) addresses both challenges by keeping raw data on devices and only exchanging model updates [1]. FL consists of a collaborative learning framework, in which repeatedly, each edge device trains on its own data for certain iterations and then uploads the model or the gradients to a central server for aggregation. However, the digital transmission of large-scale model updates still creates a communication bottleneck, especially as the number of participants scales [2]. As more and more end devices are wirelessly connected, considering FL within wireless networks is essential [3].

The work of P. Zheng, Y. Zhu and A. Schmeink was supported by BMFTR Germany in the program of “Souverän. Digital. Vernetzt.” Joint Project 6G-ANNA with project identification number 16KISK097.

Lorenz Bielefeld and Paul Zheng and co-first authors. Y. Hu is the corresponding author.

Over-the-air computation (AirComp) technique proposed in [4], [5] is investigated as a means to counter the communication bottleneck issue of FL [6], [7], [8]. By exploiting the waveform superposition of the wireless multiple-access channel, a server can directly aggregate local updates “over the air,” enabling scalability with the number of devices to participate in each communication round. One of the central design challenges in AirComp-FL is power control for signal power or amplitude alignment. The ideal aim is to obtain equally average received power from user equipments (UEs) at the base station (BS) so that a summation operation can be performed. Under average power constraints, channel inversion and threshold-based policies have been shown to minimize aggregation mean-squared error (MSE): UEs with weak channels transmit at their maximum power budget, while UEs above a threshold invert their channels [9], [10], [11].

However, the above designs ignore the instantaneous peak-power limitations due to the non-linearity of power amplifiers from a certain power level. Operating in the nonlinear region causes signal distortion and receiver misalignment. This is a common issue for orthogonal frequency-division multiplexing (OFDM), whose peak-to-average power ratio (PAPR) is known to be high. While recent works have advanced AirComp in OFDM systems [12], [13], [14], they typically optimize MSE under average-power budgets and imperfect channel state information (CSI) but do not quantify or enforce instantaneous peak-power constraints.

This paper studies AirComp-FL under both average and instantaneous peak-power constraints for single-carrier transmission and multi-carrier OFDM systems. We characterize the induced aggregation error when peaks are constrained, and evaluate the effect of practical mitigation mechanisms.

The main contributions are summarized as follows:

- We highlight the practical limitations of peak power constraint in a practical system due to the non-linear region of power amplifiers.
- We present and evaluate the most common method to handle the peak power constraints: amplitude clipping that repeatedly applies clipping, i.e., clip the time-domain peak power value that is set by the nonlinearity of the power amplifier, and filtering the out-of-band distortion. Implementation details for both multiple-access schemes are provided.
- Empirical evaluation and design insights. Evaluating under

LeNet trained on CIFAR-10, we quantify PAPR, aggregation MSE, and learning accuracy. We observe substantially high PAPR of a AirComp-FL signal, either in single-carrier or multi-carrier OFDM. Enforcing peak constraints via clipping yields accuracy degradation and may cause model divergence.

The remaining sections are organized as follows: Section II introduces the FL-OTA system models for single-carrier and multi-carrier OFDM and the associated average power allocation based on MSE minimization. Section III formalizes the instantaneous peak-power constraint and presents the clipping mechanisms. Section IV presents the simulation settings and results.

II. SYSTEM MODEL

A. Federated Learning

Consider a single-antenna BS serving a set $\mathcal{K} \triangleq \{1, \dots, K\}$ of K UEs, where FL is performed. A supervised learning task is considered for FL. UE k holds a local dataset \mathcal{D}_k of size D_k . The local empirical loss function can be written as

$$F_k(\mathbf{w}) = \frac{1}{D_k} \sum_{x \in \mathcal{D}_k} \ell(\mathbf{w}; x), \quad (1)$$

where $\ell(\mathbf{w}; x)$ denotes the loss of the prediction of the sample $x \in \mathcal{D}_k$ evaluated with model weights $\mathbf{w} \in \mathbb{R}^N$. FL has the objective of minimizing the empirical global loss function:

$$\min_{\mathbf{w} \in \mathbb{R}^N} \sum_{k \in \mathcal{K}} D_k F_k(\mathbf{w}). \quad (2)$$

Equal size of local dataset is assumed, i.e. $D_k = D$ for any $k \in \mathcal{K}$. FL consists of multiple communication rounds where t -th communication round is described as follows:

- 1) BS broadcasts the global model from previous communication round $\mathbf{w}^{(t-1)}$ to all UEs. This step is assumed without issue since BS has sufficient transmit power.
- 2) Each UE $k \in \mathcal{K}$ performs a mini-batch stochastic gradient descent step based on $\mathbf{w}^{(t-1)}$ to minimize the local empirical loss F_k over its local dataset \mathcal{D}_k . The resulting gradient vector is denoted as $\bar{\mathbf{g}}_k^{(t)}$.
- 3) When all UEs are ready for uplink transmission, a pilot signal is sent orthogonally from each UE to BS (assuming sufficient resources for short pilot signals). We assume perfect CSI at the BS as commonly assumed in the literature [8], [6]. With the channel state of each UE, BS determines the transmit power that each UE should use for AirComp, and sends the power information to each UE.
- 4) All UEs apply the same normalization that transforms $\bar{\mathbf{g}}_k^{(t)}$ to $\mathbf{g}_k^{(t)}$ so that $\mathbb{E}[\mathbf{g}_k^{(t)}] = 0$ and $\mathbb{E}[\|\mathbf{g}_k^{(t)}\|_2^2] = N$ [8], [15]:

$$\mathbf{g}_k^{(t)} = \frac{\bar{\mathbf{g}}_k^{(t)} - \mu}{\Gamma}, \quad (3)$$

where the normalizing mean $\mu^{(t)} = \frac{1}{|\mathcal{S}_c|} \sum_{k \in \mathcal{S}_c} \mu_k^{(t)}$ and standard deviation $\Gamma^{(t)} = \frac{1}{|\mathcal{S}_c|} \sum_{k \in \mathcal{S}_c} \Gamma_k^{(t)}$ are obtained by averaging the statistics of each participating clients:

$$\mu_k^{(t)} = \frac{1}{m} \sum_{i=1}^d \bar{g}_k^{(t)}[i], \quad \Gamma_k^{(t)} = \sqrt{\frac{1}{m} \sum_{i=1}^d \bar{g}_k^{(t)2}[i] - \mu_k^{(t)2}}, \quad (4)$$

where $\bar{\mathbf{g}}_k^{(t)} = (\bar{g}_k^{(t)}[i])_{i=1, \dots, N}$ the gradient vector for end-device k . Note that $\mu^{(t)}$ and $\Gamma^{(t)}$ have to be uniform across all end-devices due to the nature of AirComp and must be estimated before the data communication.

- 5) Each then sends the normalized gradient $\mathbf{g}_k^{(t)}$ via analog signal with the power control information given by BS. The results via AirComp at the BS gives the approximation of the gradient average $\tilde{\mathbf{g}}^{(t)}$:

$$\tilde{\mathbf{g}}^{(t)} \approx \bar{\mathbf{g}}^{(t)} \triangleq \frac{1}{K} \sum_{k \in \mathcal{K}} \bar{\mathbf{g}}_k^{(t)}, \quad (5)$$

(details will be shown in later section), and update the new global model $\mathbf{w}^{(t)} = \mathbf{w}^{(t-1)} - \eta \bar{\mathbf{g}}^{(t)}$ with $\eta > 0$ the learning rate and $\bar{\mathbf{g}}^{(t)}$ the de-normalized gradients.

In the following sections, we focus on step 5 that consists of the gradient transmission via AirComp techniques in single-carrier and multi-carrier OFDM-based systems. For ease of notation, the index of communication round t is removed from all notations, since the principle is identical given any channel states and gradient vectors.

B. Single-Carrier AirComp

1) *Transmission of gradient:* In the case of single-carrier transmission, each communication round is divided into N time slots, where N is the size of the trainable parameters of the neural network. In time slot $n = 1, \dots, N$, all devices transmit their n -th normalized gradient value $\mathbf{g}_k[n]$. Through the use of AirComp, the superimposed characteristics of the wireless medium are exploited to calculate the target function (5). We assume block-fading, so that the channel characteristics stay constant over the transmission of one gradient vector as assumed in most works [6], [8]. The received signal at the centralized server in a given communication round can be written as

$$\mathbf{y} = \sum_{k \in \mathcal{K}} h_k \sqrt{p_k} \mathbf{g}_k + \mathbf{n}, \quad (6)$$

with $h_k > 0$ the channel gain between BS and UE k , p_k the “average” transmit power of UE k , $\mathbf{n} \in \mathbb{R}^N$ the additive zero-mean Gaussian noise of variance σ^2 .

BS rescales the received superposed signal by a factor $\sqrt{\alpha} > 0$ and dividing by the number of UEs K , and then de-normalize the gradient to obtain the $\tilde{\mathbf{g}} \in \mathbb{R}^N$, the estimation of (5):

$$\tilde{\mathbf{g}} = \frac{\Gamma \sqrt{\alpha} \mathbf{y}}{K} + \mu. \quad (7)$$

2) *Power Control:* AirComp inevitably faces noises and errors. The power p_k and scaling factor α are controlled to minimize the MSE between the AirComp gradient $\tilde{\mathbf{g}}$ (7) and the true gradient $\bar{\mathbf{g}}$ (5) as

$$\begin{aligned} \text{MSE} &= \mathbb{E}[\|\tilde{\mathbf{g}} - \bar{\mathbf{g}}\|_2^2] \\ &= \frac{\Gamma^2}{K^2} \mathbb{E}[\|\sqrt{\alpha} \mathbf{y} - \sum_{k \in \mathcal{K}} \mathbf{g}_k\|_2^2] \\ &= \frac{\Gamma^2 N}{K^2} \left(\sum_{k \in \mathcal{K}} (h_k \sqrt{\alpha p_k} - 1)^2 + \alpha \sigma^2 \right). \end{aligned} \quad (8)$$

The equation can be derived by independence of zero-mean Gaussian noise with \mathbf{g}_k and that $\mathbb{E}[\|\mathbf{g}_k\|_2^2] = N$ and $\mathbb{E}[\mathbf{g}_k] = 0$. A similar expression with a factor $N + 1$ can also be obtained

without such assumptions on the gradient vector, which can be obtained via the Cauchy-Schwarz inequality as shown in [16].

To optimize the MSE, we optimize the term in the outer bracket subject to the average power constraint $P_{\text{avg,max}}$. The resulting optimization problem is given by

$$\begin{aligned} \min_{\alpha > 0, \{p_k\}_{k \in \mathcal{K}}} \quad & \sum_{k \in \mathcal{K}} (h_k \sqrt{\alpha p_k} - 1)^2 + \alpha \sigma^2 \\ \text{s.t.} \quad & (\forall k \in \mathcal{K}) \quad 0 \leq p_k \leq P_{\text{avg,max}}. \end{aligned} \quad (9)$$

The optimal solution to the optimization problem has been developed in [16]. Later, it was also extended to the case with non-zero-mean gradient, resulting in an additional composite misalignment error in the MSE expression in [9]. The optimal solution has a structure of a threshold-based scheme where devices with weaker channels transmit at their maximum average power $P_{\text{avg,max}}$, while those with channels exceeding the threshold use the respective channel inverting power.

Proposition 1 ([16], [9]). *Assuming $h_1 \geq h_2 \geq \dots \geq h_K$. There exists $k^* \in \mathcal{K}$ such that the optimal solution $(\alpha^*, (p_k^*)_{k \in \mathcal{K}})$ to the problem (9) satisfies that the corresponding denoising factor is given by*

$$\alpha^* = \frac{1}{P_{\text{avg,max}}} \left(\frac{\sum_{k \geq k^*} h_k}{\sum_{k \geq k^*} h_k^2 + \frac{\sigma^2}{P_{\text{avg,max}}}} \right)^2, \quad (10)$$

and the optimal average transmit power is given by

$$(\forall k \in \mathcal{K}) \quad p_k^* = \begin{cases} \frac{1}{\alpha h_k^2}, & \text{if } k < k^*, \\ P_{\text{avg,max}}, & \text{if } k \geq k^*. \end{cases} \quad (11)$$

C. Multi-Carrier OFDM-based AirComp

1) *Transmission of gradient:* In multi-carrier OFDM systems, individual values of \mathbf{g}_k are modulated on subchannels in the frequency domain by assigning one value of \mathbf{g}_k to one subchannel. Since the number of subchannels M within the system bandwidth B is typically less than the size of model parameter N , transmission spans multiple OFDM symbols. Let the OFDM symbol index be $\ell \in \mathcal{S} \triangleq \{0, \dots, L-1\}$ with $L = \lceil \frac{N}{M} \rceil$. For ℓ -th symbol, the subcarrier $m \in \mathcal{M} \triangleq \{0, \dots, M-1\}$ carries the gradient entry of index $n = \ell M + m$. Zero values are transmitted for $n \geq N$. The i -th transmitted OFDM-symbol discrete sample in the time domain of the k -th UE and ℓ -th OFDM-symbol is given by its IDFT:

$$(\forall i \in \mathcal{M}) \quad s_{k,\ell}[i] = \sum_{m=0}^{M-1} g_k[\ell M + m] b_{k,\ell M+m} e^{j \frac{2\pi m i}{M}}, \quad (12)$$

where $b_{k,\ell M+m} \in \mathbb{C}$ scales the transmitted power to mitigate the effect of the channel. The received frequency domain signal is given by the transmitted signal $s_{k,\ell}[i]$ convolved with the channel impulse response $h_{k,\ell}[i]$ with the length $C+1$. We suppose that each device transmits its gradient perfectly synchronized, so that the received signal at the sample i , such that $-C \leq i \leq M-1$ becomes

$$\begin{aligned} y[i] &= \sum_{k \in \mathcal{K}} s_{k,\ell}[i] \circledast h_{k,\ell}[i] + n[i], \\ &= \sum_{k \in \mathcal{K}} \left(\sum_{m=0}^{M-1} g_k[\ell M + m] b_{k,\ell M+m} e^{j \frac{2\pi m i}{M}} \right) \circledast h_{k,\ell}[i] + n[i], \end{aligned} \quad (13)$$

where $n[i] \sim \mathcal{CN}(0, \sigma^2 M)$ is the additive white Gaussian noise; \circledast is the circular convolution operator. To retrieve the frequency components, the receiver performs discrete Fourier transform (DFT) on the received signal. For $m \in \mathcal{M}$,

$$\begin{aligned} Y_{\ell M+m} &= \text{DFT}\{\{y[i]\}_{i \in \mathcal{M}}\}[m] \\ &= \frac{1}{M} \sum_{k \in \mathcal{K}} \sum_{i=0}^{M-1} \left(\sum_{m'=0}^{M-1} g_k[\ell M + m'] b_{k,\ell M+m'} e^{j \frac{2\pi m' i}{M}} \circledast h_{k,\ell}[i] \right. \\ &\quad \left. + n[i] \right) e^{-j \frac{2\pi m i}{M}} \\ &= \sum_{k=1}^K g_k[\ell M + m] b_{k,\ell M+m} H_{k,\ell M+m} + N[m], \end{aligned} \quad (14)$$

where $H_{k,\ell M+m} = |H_{k,\ell M+m}| e^{j \phi_{k,\ell M+m}}$ is the frequency response of $h_{k,\ell}[i]$ and $N[m] \sim \mathcal{CN}(0, \sigma^2)$ is the additive white Gaussian noise for each sub channel since the Fourier transform of a Gaussian distribution is also a Gaussian distribution with the same statistical properties. Due to the fact that each sub channel is associated with a different channel $H_{k,\ell M+m}$ in OFDM, the n -th gradient value can therefore be recovered by:

$$\begin{aligned} \tilde{g}[n] &= \frac{\Gamma \sqrt{\alpha_n} Y_n}{K} + \mu, \\ &= \frac{\Gamma \sqrt{\alpha_n}}{K} \sum_{k \in \mathcal{K}} |H_{k,n}| \sqrt{p_{k,n}} g_k[n] + \frac{\Gamma \sqrt{\alpha_n}}{K} N[n] + \mu, \end{aligned} \quad (15)$$

where $b_{k,\ell M+m}$ in (14) is substituted as $b_{k,\ell M+m} = \sqrt{p_{k,\ell M+m}} e^{-j \phi_{k,\ell M+m}}$, with $p_{k,\ell M+m}$ the transmit power of UE k at the subcarrier m when transmitting the ℓ -th symbol, and hence already includes the phase offset caused by the channel and $\alpha_n > 0$ is the denoising factor for the corresponding subcarrier.

2) *Power Allocation:* As for single-carrier, the power allocation is done by minimizing the MSE of each gradient value. The MSE of the gradient value n has the following expression:

$$\begin{aligned} \text{MSE}_n &= \mathbb{E}[\|\tilde{g}[n] - \bar{g}[n]\|^2] \\ &= \frac{\Gamma^2}{K^2} \left(\sum_{k \in \mathcal{K}} (|H_{k,n}| \sqrt{\alpha_n p_{k,n}} - 1)^2 + \alpha_n \sigma^2 \right), \end{aligned} \quad (16)$$

For any OFDM-symbol ℓ , the optimal power allocation for gradient values of indices $n = \ell M + m$ with $m = 0, \dots, M-1$ can be given as:

$$\min_{\alpha_{\ell} \geq 0} \sum_{m=0}^{M-1} \text{MSE}_{\ell M+m}(\alpha_{\ell M+m}, \mathbf{p}_{\ell M+m}) \quad (17a)$$

$$\text{s.t. } (\forall k \in \mathcal{K}) \quad \sum_{m=0}^{M-1} p_{k,\ell M+m} \leq P_{\text{avg,max}}, \quad (17b)$$

$$(\forall k \in \mathcal{K}) \quad (\forall m \in \mathcal{M}) \quad p_{k,\ell M+m} \geq 0, \quad (17c)$$

with $\alpha_{\ell} = (\alpha_{\ell M+m})_{m \in \mathcal{M}}$ and $\mathbf{p}_n = (p_{k,n})_{k \in \mathcal{K}}$ for any $n = \ell M + m$. This problem has been analyzed in [13] that requires a subgradient solver and partly in [14] that considers an equal α for all subcarriers.

Due to the short time frame that the power needs to be allocated, only low-complexity solution is practically feasible. Since transmit power at the UE side is typically low, we pick up the classical empirical observations that the power allocation for uplink multi-carrier OFDM has a marginal effect on the performance [17], [18]. Assuming equal power allocated to

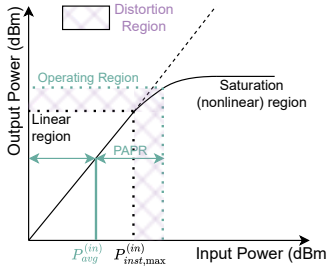


Fig. 1. Typical input and output power characteristics curve for a power amplifier.

each subcarrier for each UE, i.e., replacing the constraint (17b) by $(\forall k \in \mathcal{K}) (\forall m \in \mathcal{M}) p_{k,\ell M+m} \leq \frac{P_{\text{avg,max}}}{M}$. (18)

The problem can therefore be decoupled for each subcarrier m , and the optimal solution for each subcarrier m given a symbol ℓ , i.e., given $(H_{k,\ell M+m})_{k \in \mathcal{K}}$, $P_{\text{avg,max}}/M$ as the maximum average transmit power, and σ^2 as the noise power level, can be calculated again with Proposition 1.

III. INSTANTANEOUS PEAK POWER CONSTRAINT

Practical radio-frequency power amplifiers operate linearly only up to certain input power [19], [20]. Given a certain average power as input $P_{\text{avg}}^{(in)}$, the actual operating region would be between zero and the maximum peak instantaneous input power which can be obtained by multiplying $P_{\text{avg}}^{(in)}$ with PAPR (addition in dB domain), as illustrated in Fig. 1. Operating in nonlinear region leads to signal distortions, resulting in strong in-band and out-of-band distortions (details see later), which is to be avoided. Note that all previously determined powers are actually output powers, but can be easily converted to the input power by a one-to-one relationship. We denote $p_k^{(in)}$ and $b_{k\ell M+m}^{(in)}$ respectively the corresponding input power of p_k and $b_{k\ell M+m}$. We model this by an instantaneous amplitude limit $A_{\text{max}} > 0$ that corresponds equivalently to the input peak-power limit $P_{\text{inst,max}}^{(in)} = A_{\text{max}}^2$. The transmitted time-domain waveform $X(t)$ generated at a UE must satisfy

$$|X(t)|^2 \leq P_{\text{inst,max}}^{(in)} = A_{\text{max}}^2. \quad (19)$$

A. Peak-to-Average Power Ratio

This limitation directly interacts with the PAPR of the transmitted waveform as illustrated in Fig. 1. A low PAPR can keep the operating region within the linear region.

a) *Single-carrier transmission*: With the gradient normalization in Section II, the average per-communication round transmit power equals the configured average power budget. The peaks for single carrier transmission are directly determined by the gradient values. The k -th UE transmits the real-valued sample $g_k[n]$ matching the amplitude of waveform. Its PAPR is

$$\text{PAPR}_k = \frac{\max_n |g_k[n]|^2}{\frac{1}{N} \sum_{n=1}^N |g_k[n]|^2}. \quad (20)$$

b) *Multi-carrier OFDM transmission*: The time-domain signal for multi-carrier OFDM can be written as

$$s_{k,\ell}(t) = \sum_{m=0}^{M-1} g_k[\ell M + m] b_{k,\ell M+m} e^{j \frac{2\pi m t}{M}}. \quad (21)$$

The ideal PAPR is denoted as

$$\text{PAPR}_{k,\ell}^{\text{ideal}} = \frac{\max_t |s_{k,\ell}(t)|^2}{\frac{1}{T} \int_0^T |s_{k,\ell}(t)|^2 dt}. \quad (22)$$

In practice, only digital discrete samples can be employed to estimate PAPR. It has been shown that samples sampled at Nyquist rate inaccurately captures PAPR.

Oversampling: To accurately capture PAPR in the time-domain OFDM signal, oversampling is essential. An oversampling factor L_{os} (typically $L_{\text{os}} = 4$ is sufficient [21]) is applied by zero-padding the frequency-domain signal before the IDFT. The oversampled time-domain signal is generated as:

$$s_{k,\ell}^{(\text{os})}[i] = \sum_{m=0}^{L_{\text{os}}M-1} G_{k,\ell}[m] e^{j \frac{2\pi m i}{L_{\text{os}}M}}, \quad i = 0, \dots, L_{\text{os}}M-1, \quad (23)$$

where the zero-padded frequency-domain vector is defined as:

$$G_{k,\ell}[m] = \begin{cases} g_k[\ell M + m] b_{k,\ell M+m}^{(in)}, & 0 \leq m < M, \\ 0, & M \leq m < L_{\text{os}}M. \end{cases} \quad (24)$$

The per-symbol PAPR can therefore be estimated as

$$\text{PAPR}_{k,\ell} = \frac{\max_i |s_{k,\ell}^{(\text{os})}[i]|^2}{\frac{1}{L_{\text{os}}M} \sum_{i=0}^{L_{\text{os}}M-1} |s_{k,\ell}^{(\text{os})}[i]|^2}. \quad (25)$$

B. Clipping with Oversampling

The commonly used technique to deal with the high PAPR issue is applying the procedure of iterative clipping-and-filtering (ICF). Since clipping results in in-band and out-of-band distortions in multi-carrier OFDM [19], [20]. A low-pass filter is applied afterwards to limit out-of-band distortion, which may result in the rise of PAPR, necessitating repeated such procedures.

Amplitude Clipping: Let $\mathcal{C}_{A_{\text{max}}}(x) \triangleq \min\{1, A_{\text{max}}/|x|\} x$ denote the time-sample-wise amplitude clipper.

1) *Single-carrier*: Each UE transmits

$$x_k[n] = \mathcal{C}_{A_{\text{max}}}(\sqrt{p_k^{(in)}} g_k[n]) = \min\left\{1, \frac{A_{\text{max}}}{\sqrt{p_k^{(in)}} g_k[n]}\right\} \sqrt{p_k^{(in)}} g_k[n]. \quad (26)$$

In single-carrier, this is equivalent to considering the transmission of a clipped version of the gradient values, with nothing else altered by the clipping.

2) *Multi-Carrier OFDM*:

a) *Amplitude Clipping*: For each OFDM symbol ℓ , the oversampled complex time-domain samples are clipped while preserving phase:

$$x_{k,\ell}^{(\text{os})}[i] = \mathcal{C}_{A_{\text{max}}}(s_{k,\ell}^{(\text{os})}[i]) = \min\left\{1, \frac{A_{\text{max}}}{|s_{k,\ell}^{(\text{os})}[i]|}\right\} s_{k,\ell}^{(\text{os})}[i]. \quad (27)$$

Since the clipping operation is nonlinear, distortions are inevitable. The clipping distortion in the time domain can be written as: $d_{k,\ell}^{(\text{os})}[i] = x_{k,\ell}^{(\text{os})}[i] - s_{k,\ell}^{(\text{os})}[i]$.

b) *Frequency-Domain Distortion*: Transforming the clipped signal back to the frequency domain via DFT yields:

$$X_{k,\ell}[m] = \text{DFT}\{x_{k,\ell}^{(\text{os})}[i]\}[m] = G_{k,\ell}[m] + D_{k,\ell}[m], \quad (28)$$

where $D_{k,\ell}[m] = \text{DFT}\{d_{k,\ell}^{(\text{os})}[i]\}[m]$ represents the clipping distortion in the frequency domain.

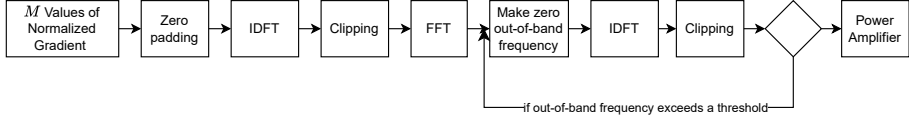


Fig. 2. Flow Diagram for ICF in multi-carrier OFDM systems.

This distortion consists of two components:

- **In-band distortion:** distortion on the considered subcarriers $m \in \mathcal{M}$, which degrades the aggregated gradients.
- **Out-of-band emissions:** spectral regrowth on the zero-padded subcarriers $M \leq m < L_{os}M$ due to clipping, which causes interference to adjacent channels.

c) *Filtering*: To suppress out-of-band emissions, a low-pass filter is applied. Define a rectangular filter:

$$H_{\text{filter}}[m] = \begin{cases} 1, & 0 \leq m < M, \\ 0, & M \leq m < L_{os}M. \end{cases} \quad (29)$$

The filtered frequency-domain signal is:

$$X_{k,\ell}^{(\text{filt})}[m] = X_{k,\ell}[m] \cdot H_{\text{filter}}[m]. \quad (30)$$

Converting back to the time domain yields the filtered signal:

$$x_{k,\ell}^{(\text{filt})}[i] = \text{IDFT}\{X_{k,\ell}^{(\text{filt})}[m]\}[i]. \quad (31)$$

However, filtering may reintroduce peak regrowth, as it restores some of the constructive interference among subcarriers that clipping had disrupted [19].

d) *Iterative Clipping and Filtering*: To jointly control PAPR and out-of-band emissions, an ICF procedure is commonly employed [22]. The algorithm proceeds as follows for each symbol ℓ :

- 1) Initialize: $x_{k,\ell}^{(0)}[i] = s_{k,\ell}^{(\text{os})}[i]$; $j = 1$.
- 2) While $x_{k,\ell}^{(j,\text{clip})}[i]$ has out-of-band distortion higher than a threshold:
 - a) Clip: $x_{k,\ell}^{(j,\text{clip})}[i] = \mathcal{C}_{A_{\text{max}}}(x_{k,\ell}^{(j-1)}[i])$.
 - b) DFT: $X_{k,\ell}^{(j)}[m] = \text{DFT}\{x_{k,\ell}^{(j,\text{clip})}[i]\}[m]$.
 - c) Filter: $X_{k,\ell}^{(j,\text{filt})}[m] = X_{k,\ell}^{(j)}[m] \cdot H_{\text{filter}}[m]$.
 - d) IDFT: $x_{k,\ell}^{(j)}[i] = \text{IDFT}\{X_{k,\ell}^{(j,\text{filt})}[m]\}[i]$.
- 3) Output: $x_{k,\ell}^{(\text{ICF})}[i] = x_{k,\ell}^{(J_{\text{max}})}[i]$.

The final transmitted signal is $x_{k,\ell}^{(\text{ICF})}[i]$, which satisfies the peak-power constraint with a certain threshold for out-of-band distortion. The flow diagram of the whole procedure can be found in Fig. 2.

IV. SIMULATIONS

A. Simulation Settings

In the simulations the LeNet convolutional neural network with 62006 trainable parameters is trained on the Cifar-10 dataset for 500 communication rounds, where the data is independent and identically distributed among $K = 40$ UEs. The learning rate is set to 1, while the local batch size is set to 256 during the training. In each communication round all UEs participate and are uniformly distributed on a 100 meter radius disk around the base station. As a large-scale fading model, the free-space-path loss is used, which is combined with Rayleigh fading as a small-scale fading model. The constraint of the maximum average power $P_{\text{avg},\text{max}}$ of UEs is chosen to be

23 dBm, while the constraint of the the maximum instantaneous power $P_{\text{inst},\text{max}}$ is chosen to be 26 dBm. In multi-carrier OFDM transmission, $M = 32$ subcarriers are used in order to reduce OFDM complexity, where each subcarrier transmits with a bandwidth of 60 kHz. The iterative clipping and filtering is done until the out-of-band emissions are below -10 dBm. For the single carrier transmission, a bandwidth of 60 kHz is used. Oversampling ratio is taken as $L_{os} = 4$ as in [21].

B. Simulation Results and Discussions

All curves in this section are smoothed for readability.

PAPR is shown in Fig. 3. Without clipping, the PAPR is high (about 35 dB), while after clipping and filtering, the PAPR remains close to 15 dB. Note that the results without clipping and before clipping are different since PAPR depends on the actual values to be transmitted and clipping and filtering procedure changes the actual values to approximate the average of gradient (5). We also observe that single-carrier transmission can exhibit higher PAPR than multi-carrier OFDM transmission, which is unusual for digital modulation schemes. This stems from the nature of amplitude modulation (for the single-carrier case), where the power is directly related to the actual values to be transmitted, which can actually go up to “infinity” if the gradient values can take arbitrarily large values. The decrease in PAPR in the single-carrier case w.r.t. communication rounds may be due to that the model has been well trained, so the gradient values divergence is smaller.

The approximation error for (5), i.e. the MSE in (8) and (16), is shown in Fig. 4. The true squared error (TSE) is defined as $\frac{1}{N} \sum_{n=1}^N \|\tilde{g}[n] - \bar{g}[n]\|^2$. Clipping increases the TSE relative to the non-clipping baseline, and the analytical MSE underestimates the TSE. Interestingly, for multi-carrier OFDM, the post-clipping TSE is larger when the noise power is lower. The reason is that, at low noise, the scaling factors α_n take larger values, therefore amplifying the in-band distortion caused by ICF, resulting in higher error.

The results on FL test accuracy are shown in Fig. 5. For single-carrier (Fig. 5a), we observe consistent but small gaps between clipped and unclipped cases, with higher noise yielding lower accuracy overall. A noticeable accuracy drop appears at around 50 communication rounds for the clipped case. For multi-carrier OFDM (Fig. 5b), as predicted by the TSE, the clipped case performs worse at lower noise; at $\sigma_n^2/\text{Hz} = -110$ dBm/Hz, training may even diverge. The corresponding accuracy loss due to clipping (considering the peak power constraint) is shown in Fig. 6. At the later stage of training, the loss of test accuracy is about 1.5–2%, while around 50 rounds it can peak at up to 8% for the drop of accuracy mentioned previously.

V. CONCLUSION

This work highlights an overlooked practical issue in Air-Comp-FL: the instantaneous peak power constraint imposed

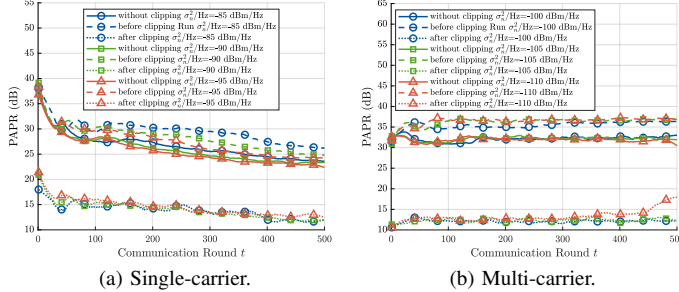


Fig. 3. Peak-to-average power ratio (PAPR) w.r.t. communication rounds.

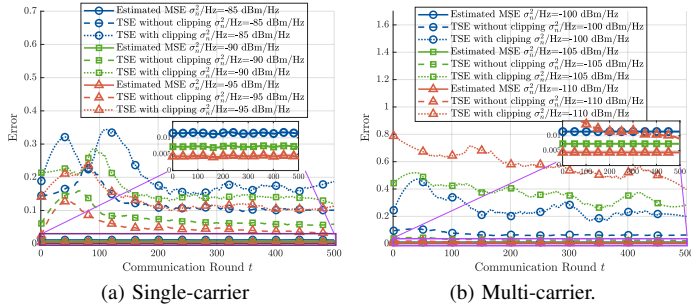


Fig. 4. Error of the approximated average gradient w.r.t. the actual average gradient. TSE denotes the *True Square Error*; Estimated MSE is given by (8) and (16).

by the nonlinearity in power amplifiers. This is an issue in AirComp-FL since it uses analog transmission and some works consider multi-carrier OFDM transmissions. We applied the classic PAPR reduction methods of iterative amplitude clipping and frequency-domain filtering. Enforcing peak power constraint can indeed degrade aggregation and final accuracy, in some cases, the effects are marginal, and in some other cases (multi-carrier with low noise level), cause divergence. Counter-intuitively, the impact is stronger at lower noise for multi-carrier OFDM because the scaling factor from optimization is higher and therefore the in-band distortion is too much amplified. This work should motivate further research in peak power constraint-aware power control and better PAPR reduction techniques for single-carrier and multi-carrier AirComp-FL systems.

REFERENCES

- [1] H. B. McMahan, E. Moore, D. Ramage, S. Hampson, and B. A. Y. Arcas, “Communication-efficient learning of deep networks from decentralized data,” in *AISTATS*, Fort Lauderdale, Florida, USA, 2017.
- [2] J. Konečný, H. B. McMahan, F. X. Yu, P. Richtárik, A. T. Suresh, and D. Bacon, “Federated learning: Strategies for improving communication efficiency,” 2017, arXiv:1610.05492.
- [3] W. Y. B. Lim, N. C. Luong, D. T. Hoang, Y. Jiao, Y.-C. Liang, Q. Yang, D. Niyato, and C. Miao, “Federated learning in mobile edge networks: A comprehensive survey,” *IEEE Commun. Surv. & Tut.*, vol. 22, no. 3, pp. 2031–2063, 2020.
- [4] B. Nazer and M. Gastpar, “Computation over multiple-access channels,” *IEEE Trans. Inf. Theory*, vol. 53, no. 10, pp. 3498–3516, 2007.
- [5] M. Goldenbaum and S. Stańczak, “Robust analog function computation via wireless multiple-access channels,” *IEEE Trans. Commun.*, vol. 61, no. 9, pp. 3863–3877, 2013.
- [6] K. Yang, T. Jiang, Y. Shi, and Z. Ding, “Federated learning via over-the-air computation,” *IEEE Trans. Wireless Commun.*, vol. 19, no. 3, pp. 2022–2035, 2020.
- [7] M. M. Amiri and D. Gündüz, “Machine learning at the wireless edge: Distributed stochastic gradient descent over-the-air,” *IEEE Trans. Signal Process.*, vol. 68, pp. 2155–2169, 2020.
- [8] G. Zhu, Y. Wang, and K. Huang, “Broadband analog aggregation for low-latency federated edge learning,” *IEEE Trans. Wireless Commun.*, vol. 19, no. 1, pp. 491–506, 2020.
- [9] N. Zhang and M. Tao, “Gradient statistics aware power control for over-the-air federated learning,” *IEEE Trans. Wireless Commun.*, vol. 20, no. 8, pp. 5115–5128, 2021.
- [10] X. Cao, G. Zhu, J. Xu, and S. Cui, “Transmission power control for over-the-air federated averaging at network edge,” *IEEE J. Sel. Areas Commun.*, vol. 40, no. 5, pp. 1571–1586, 2022.
- [11] X. Cao, G. Zhu, J. Xu, Z. Wang, and S. Cui, “Optimized power control design for over-the-air federated edge learning,” *IEEE J. Sel. Areas Commun.*, vol. 40, no. 1, pp. 342–358, 2022.
- [12] N. G. Evgenidis, S. A. Tegos, P. D. Diamantoulakis, and G. K. Karagiannidis, “Over-the-Air Computing in OFDM Systems,” *IEEE Commun. Lett.*, vol. 28, no. 11, pp. 2523–2527, Nov. 2024.
- [13] Y. Chen, H. Xing, J. Xu, L. Xu, and S. Cui, “Over-the-air computation in OFDM systems with imperfect channel state information,” *IEEE Trans. Commun.*, vol. 72, no. 5, pp. 2929–2944, 2024.
- [14] X. Xie, C. Hua, J. Hong, and W. Xu, “Optimal power control and CSI acquisition for over-the-air computation in OFDM system,” *IEEE Trans. Wireless Commun.*, vol. 23, no. 6, pp. 6533–6545, Jun. 2024.
- [15] P. Zheng, Y. Zhu, M. Bouchaala, Y. Hu, S. Stanczak, and A. Schmeink, “Federated learning with integrated over-the-air computation and sensing in IRS-assisted networks,” in *WSA*, Braunschweig, Germany, 2023.
- [16] X. Cao, G. Zhu, J. Xu, and K. Huang, “Optimized power control for over-the-air computation in fading channels,” *IEEE Transactions on Wireless Communications*, vol. 19, no. 11, pp. 7498–7513, 2020.
- [17] K. Kim, Y. Han, and S.-L. Kim, “Joint subcarrier and power allocation in uplink OFDMA systems,” *IEEE Commun. Lett.*, vol. 9, no. 6, pp. 526–528, 2005.
- [18] E. Yaacoub, H. Al-Asadi, and Z. Dawy, “Low complexity scheduling algorithms for the LTE uplink,” in *IEEE Symp. Comp. and Commun.*, 2009, pp. 266–270.
- [19] S. H. Han and J. H. Lee, “An overview of peak-to-average power ratio reduction techniques for multicarrier transmission,” *IEEE Wireless Commun.*, vol. 12, no. 2, pp. 56–65, 2005.
- [20] Y. Rahmatallah and S. Mohan, “Peak-to-average power ratio reduction in OFDM systems: A survey and taxonomy,” *IEEE Commun. Surv. & Tut.*, vol. 15, no. 4, pp. 1567–1592, 2013.
- [21] C. Tellambura, “Computation of the continuous-time PAR of an OFDM signal with BPSK subcarriers,” *IEEE Commun. Lett.*, vol. 5, no. 5, pp. 185–187, 2001.
- [22] J. Armstrong, “Peak-to-average power reduction for OFDM by repeated clipping and frequency domain filtering,” *Electronics Letters*, vol. 38, pp. 246–247, 2002.

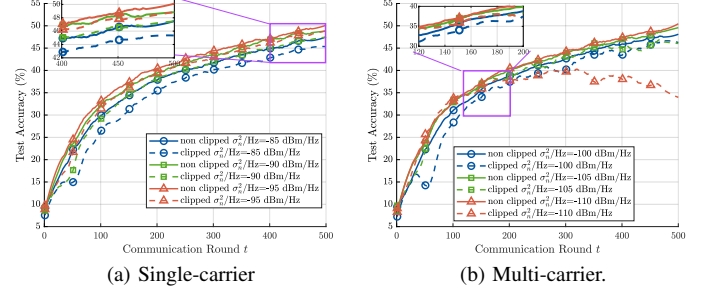


Fig. 5. Test Accuracy w.r.t. communication rounds.

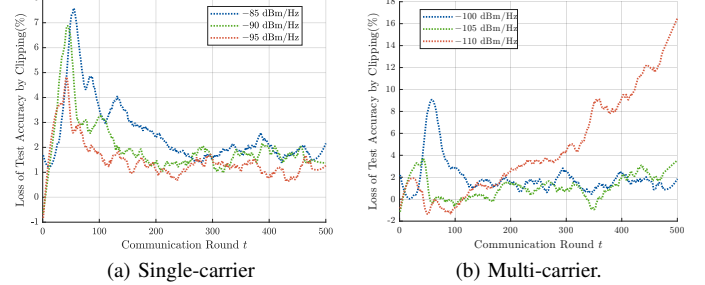


Fig. 6. Loss of test accuracy by imposing the peak power constraint (after clipping and filtering).